

# Recovery of monoclinic phase of VO<sub>2</sub> nanoparticles from oxidized samples: Assessment of reusability and optimization of re-annealing conditions

Ho Nguyen Hong Tham<sup>1</sup>, Nguyen Thi Thanh Nhan<sup>1</sup>, Nguyen Thi Tuong Vy<sup>1</sup>,  
Le Phuong Thao<sup>1</sup>, Le Thi My Nhi<sup>2</sup>, Hoang Thi Hang<sup>2,3</sup>, Le Thi Ngoc Loan<sup>2,\*</sup>

<sup>1</sup>Faculty of Education, Quy Nhon University, Vietnam

<sup>2</sup>Faculty of Natural Sciences, Quy Nhon University, Vietnam

<sup>3</sup>Quantum Solid State Physics, Department of Physics and Astronomy, KU Leuven, Belgium

Received: 27/02/2026; Revised: 24/03/2026;

Accepted: 25/03/2026; Published: 28/06/2026

## ABSTRACT

Vanadium dioxide (VO<sub>2</sub>) nanoparticles in the monoclinic (M) phase exhibit a reversible metal–insulator transition (MIT) at ~68 °C, underpinning thermochromic applications such as smart windows and thermal sensors. However, prolonged atmospheric exposure causes progressive surface oxidation that converts V<sup>4+</sup> to V<sup>5+</sup>, leading to phase degradation and loss of thermochromic function. This study demonstrates that oxidized VO<sub>2</sub> nanopowders can be fully recovered by thermal re-annealing in an inert argon atmosphere. Starting from VO<sub>2</sub>(M) nanoparticles synthesized via a hydrothermal route, controlled oxidation under ambient conditions produced a degraded sample rich in V<sub>2</sub>O<sub>5</sub>. Systematic re-annealing at 450–600 °C for 2–3 h was investigated to identify the optimal recovery conditions. XRD, Raman spectroscopy, and UV-Vis-NIR transmittance measurements confirm complete phase restoration and recovery of thermochromic switching performance equivalent to that of the as-synthesized material, establishing a practical strategy for reusing degraded VO<sub>2</sub> nanopowder stocks.

**Keywords:** Vanadium dioxide, smart window, transition material, thermochromic recovery.

## 1. INTRODUCTION

Vanadium dioxide (VO<sub>2</sub>) is a polymorphic transition-metal oxide capable of adopting several crystal structures—monoclinic (M), VO<sub>2</sub>(A), VO<sub>2</sub>(B), and VO<sub>2</sub>(D) - despite sharing the same chemical composition [1] - [3]. The differences among these polymorphs arise from distinct VO<sub>6</sub> octahedral arrangements within the crystal lattice, giving each phase unique structural and electronic properties (Figure 1).

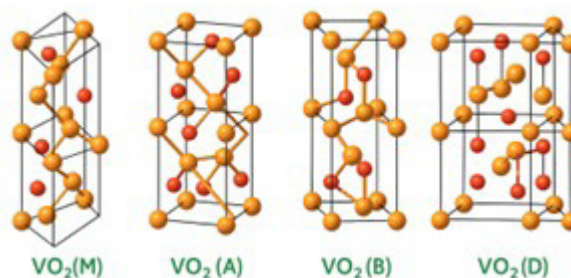


**Figure 1.** Crystal lattice structures of the four VO<sub>2</sub> polymorphs: VO<sub>2</sub>(M), VO<sub>2</sub>(A), VO<sub>2</sub>(B), and VO<sub>2</sub>(D). Orange: V atoms; red: O atoms.

\*Corresponding author:

Email: lethingocloan@qnu.edu.vn

Among these, monoclinic  $\text{VO}_2(\text{M})$  is thermodynamically stable at room temperature and is of exceptional importance owing to its reversible semiconductor-metal phase transition near 340 K ( $\sim 68^\circ\text{C}$ ), first reported by Morin [4]. In the monoclinic state, vanadium atoms form paired dimers along the c-axis, opening a band gap and yielding semiconducting behavior. Upon heating, dimerization disappears, the density of states near the Fermi level increases sharply, and metallic conductivity is recovered [4] - [5]. This structural reorganization also reverses the optical response: below the transition temperature,  $\text{VO}_2$  transmits near-infrared (NIR) radiation; above it, the metallic phase strongly reflects NIR light [6] - [7]. This reversible electro-optical switching underpins thermochromic smart windows, thermal sensors, and optical limiters.

A variety of synthesis strategies have been developed for  $\text{VO}_2$ , including physical vapor deposition, magnetron sputtering, sol-gel, and hydrothermal methods [8] - [9]. Hydrothermal synthesis is particularly attractive because it permits direct control of crystal phase, particle size, and morphology through adjustment of temperature, pH, and redox atmosphere [10] - [11]. Typically, a  $\text{V}^{5+}$  precursor such as  $\text{V}_2\text{O}_5$  is reduced to  $\text{V}^{4+}$  under hydrothermal conditions, yielding metastable  $\text{VO}_2(\text{B})$  or  $\text{VO}_2(\text{A})$  that is subsequently annealed to phase-pure  $\text{VO}_2(\text{M})$  in an inert atmosphere [10] - [12].

Despite extensive research, the storage stability of synthesized  $\text{VO}_2$  nanopowders remains a practical challenge. Even in nominally sealed environments, prolonged ambient exposure causes gradual surface oxidation of  $\text{V}^{4+}$  to  $\text{V}^{5+}$ , forming  $\text{V}_2\text{O}_5$ -rich surface layers that broaden the MIT, reduce thermochromic contrast, and impair switching performance [1] - [13]. The nanoscale morphology of these particles accelerates this degradation relative to bulk material owing to high surface-to-volume ratios. Recovery of degraded  $\text{VO}_2$  nanopowders by thermal re-annealing in inert or reducing

atmospheres has been proposed [12] - [14], yet systematic optimization of re-annealing conditions for nanopowder specimens remains sparse in the literature.

In the present work, we synthesized  $\text{VO}_2(\text{M})$  nanoparticles by a hydrothermal route, intentionally oxidized them under ambient conditions, and conducted systematic re-annealing in argon across temperatures of  $450\text{--}600^\circ\text{C}$  and durations of 2–3 h. XRD, Raman spectroscopy, and UV-Vis-NIR transmittance measurements are used to track phase evolution and verify restoration of thermochromic function. Our results identify  $500^\circ\text{C}$  for 2 h as the optimal condition, demonstrating a straightforward, cost-effective protocol for reusing degraded  $\text{VO}_2$  nanoparticle batches.

## 2. EXPERIMENTAL SECTION

### 2.1. Materials

Vanadium pentoxide ( $\text{V}_2\text{O}_5$ ,  $\geq 98\%$ ), concentrated sulfuric acid ( $\text{H}_2\text{SO}_4$ , 98%), hydrazine hydrate ( $\text{N}_2\text{H}_4\cdot\text{H}_2\text{O}$ , 50–60%), sodium hydroxide ( $\text{NaOH}$ ,  $\geq 95\%$ ), polyvinylpyrrolidone (PVP, MW = 40,000 g/mol), and absolute ethanol (99.6%) were used as received. Deionized (DI) water was used throughout.

### 2.2. Synthesis of $\text{VO}_2(\text{M})$ nanoparticles

$\text{VO}_2(\text{M})$  nanoparticles were prepared via a four-step hydrothermal procedure illustrated in Figure 2.

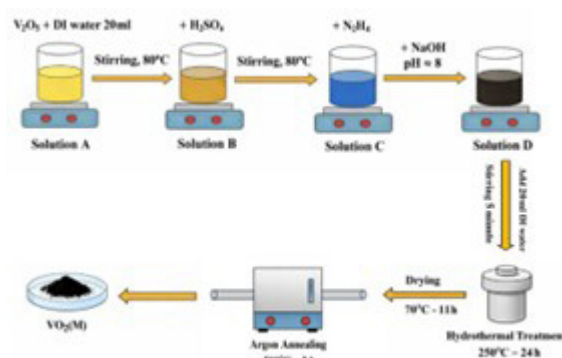


**Figure 2.** Schematic of the hydrothermal synthesis route for  $\text{VO}_2(\text{M})$  nanoparticles, from  $\text{V}_2\text{O}_5$  precursor dissolution to argon annealing.

Step 1: Precursor preparation: 0.9 g of  $V_2O_5$  was dispersed in 20 mL DI water under stirring at 60 °C (Solution A, yellow suspension). Then 1.5 mL of  $H_2SO_4$  was added dropwise at 80 °C to give a deep-yellow solution (Solution B).

Step 2: Reduction and pH adjustment: 0.5 mL of  $N_2H_4$  was introduced dropwise, raising the temperature to 90–100 °C and yielding a blue solution (Solution C, pH  $\approx$  0.8-1). NaOH (2.3 g) was then added to adjust pH to  $\sim$ 8, producing a dark-brown suspension (Solution D). The color evolution is shown in Figure 3.

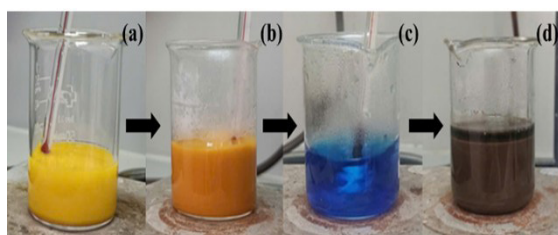


**Figure 3.** Optical photographs of the precursor at each synthesis step: (a) yellow  $V_2O_5$  suspension; (b) deep-yellow Solution B; (c) blue Solution C after  $N_2H_4$  reduction; (d) dark-brown Solution D after pH adjustment.

Step 3: Hydrothermal treatment: the precursor was transferred to a 25 mL Teflon-lined stainless-steel autoclave and heated at 250 °C for 24 h (5 °C  $min^{-1}$ ).

Step 4: Post-treatment and annealing: the black precipitate was washed twice with DI water and once with ethanol, dried at 70 °C for 11 h, then annealed at 500 °C for 2 h in flowing Ar (10 °C  $min^{-1}$ ) to obtain phase-pure  $VO_2(M)$ .

### 2.3. Controlled oxidation

Synthesized  $VO_2(M)$  powders were stored in an open beaker under ambient laboratory conditions ( $\sim$ 25 °C, relative humidity 60–70%) for a controlled period (1 week) to simulate real-world aging. Color changes were recorded photographically.

### 2.4. Recovery by re-annealing

Oxidized powders were re-annealed in a tube furnace under continuous Ar flow. Stage 1 (temperature optimization): re-annealing at 450,

500, 550, and 600 °C for 2 h. Stage 2 (duration optimization): re-annealing at 500 °C for 2 h and 3 h. All heating ramps were 10 °C  $min^{-1}$ .

### 2.5. Characterization

The crystal structure of the samples was determined by X-ray diffraction using a D2 Phaser diffractometer (Bruker, Rheinstetten, Germany) equipped with a Cu  $K\alpha$  radiation source ( $\lambda = 1.54 \text{ \AA}$ ). Raman spectra were acquired using a Horiba XPLora Plus spectrometer (Horiba, Villeneuve d'Ascq, France) with a 532 nm laser excitation. The surface morphology was examined using a JSM-IT200 scanning electron microscope (JEOL, Japan). Thermochromic performance was evaluated by UV-Vis-NIR transmittance spectroscopy over a range of 300 – 2000 nm using a JASCO V-770 spectrophotometer (JASCO, Hachioji, Japan) equipped with a temperature-controlled stage during heating and cooling cycles between 30 and 100 °C.

## 3. RESULTS AND DISCUSSION

### 3.1. As-synthesized $VO_2(M)$ nanoparticles

The hydrothermal synthesis and Ar annealing steps produced a jet-black powder (Figure 4, right), in stark visual contrast to the yellow  $V_2O_5$  precursor (Figure 4, left). The color change reflects successful  $V^{5+} \rightarrow V^{4+}$  reduction and  $VO_2(M)$  phase formation.



Photograph of yellow  $V_2O_5$  powder

Photograph of black  $VO_2(M)$  powder

**Figure 4.** Optical photographs of the yellow  $V_2O_5$  precursor powder (left) and the as-synthesized black  $VO_2(M)$  nanoparticle powder (right).

The UV-Vis-NIR transmittance spectra of original sample (Figure 5) show a pronounced divergence between the 30 °C (semiconducting) and 100 °C (metallic) curves in the NIR region (800 - 2000 nm), confirming active

thermochromic switching through the MIT at  $\sim 68^\circ\text{C}$  [15]. This large NIR transmittance contrast is the key functional signature of high-quality  $\text{VO}_2(\text{M})$ .

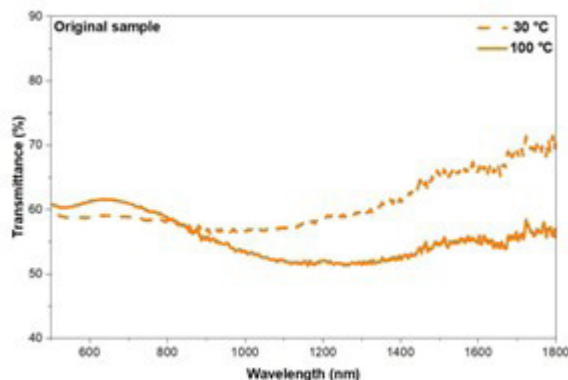


**Figure 5.** UV-Vis-NIR transmittance spectra of as-synthesized  $\text{VO}_2(\text{M})$  film (Original sample) at  $30^\circ\text{C}$  (dashed line) and  $100^\circ\text{C}$  (solid line), showing clear thermochromic NIR switching.

### 3.2. Oxidation behavior under ambient conditions

When  $\text{VO}_2(\text{M})$  powder was stored in an open beaker under ambient air (Figure 6), a progressive color transformation was observed over the course of days to weeks: black  $\rightarrow$  bluish-black  $\rightarrow$  moss green  $\rightarrow$  dark moss green (Figure 7a). This sequence mirrors the gradual oxidation of  $\text{V}^{4+}$  to  $\text{V}^{5+}$  and accumulation of  $\text{V}_2\text{O}_5$ -like surface species. The SEM image in Figure 7b reveals that re-annealing at  $500^\circ\text{C}$  for 3 hours resulted in a mixed morphology, consisting predominantly of nanoparticles with a partial formation of nanorods.

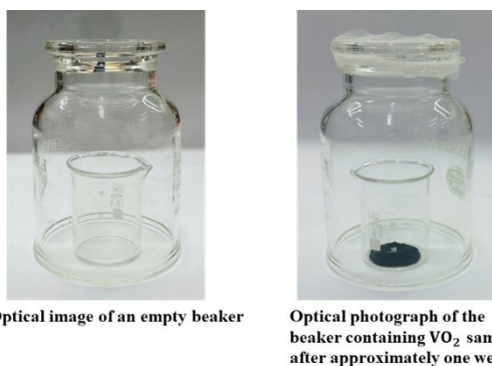


**Figure 6.** Storage experiment: empty reference beaker (left) and  $\text{VO}_2$  powder sample after  $\sim$ one week of ambient air exposure (right).

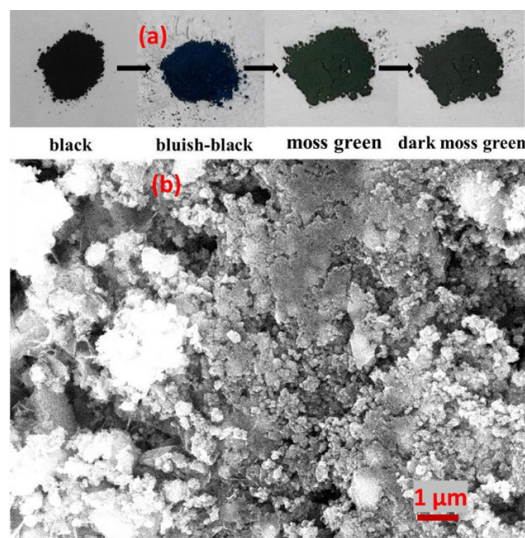


**Figure 7.** Time-dependent color evolution of  $\text{VO}_2$  powder during ambient oxidation: black  $\rightarrow$  bluish-black  $\rightarrow$  moss green  $\rightarrow$  dark moss green (a) and SEM image of the recovery sample annealed at  $500^\circ\text{C}$  in 3h.

XRD analysis of the oxidized sample (Figure 8) reveals emergence of  $\text{V}_2\text{O}_5$  reflections alongside diminished  $\text{VO}_2(\text{M})$  peaks, confirming phase transformation rather than mere surface contamination [16]. The original sample (orange) displays only sharp  $\text{VO}_2(\text{M})$  reflections, while the oxidized sample (cyan) shows clear additional peaks at positions characteristic of  $\text{V}_2\text{O}_5$  at 2 theta positions of  $26.2^\circ$ ,  $31^\circ$ ,  $32.4^\circ$ ,  $41^\circ$ ,  $52^\circ$  and  $62^\circ$ . Nevertheless, the persistence of lower-intensity peaks at  $27.9^\circ$ ,  $37^\circ$ ,  $55^\circ$ ,  $65^\circ$  and  $70^\circ$  indicates a residual  $\text{VO}_2(\text{M})$  component. Furthermore, the diffractogram suggests the secondary presence of the  $\text{VO}_2(\text{B})$  phase as an impurity.

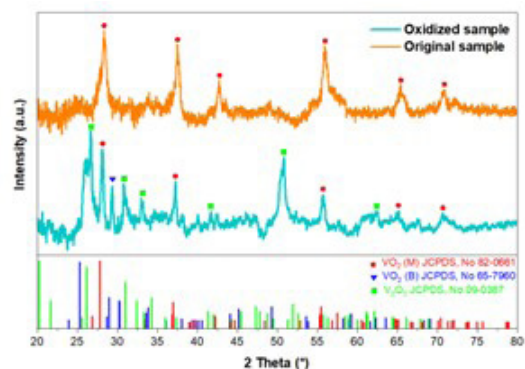


**Figure 8.** XRD patterns of the original  $\text{VO}_2(\text{M})$  (orange) and oxidized sample (cyan) compared with reference stick patterns for  $\text{VO}_2(\text{B})$  (blue),  $\text{V}_2\text{O}_5$  (green) and  $\text{VO}_2(\text{M})$  (red). Dashed lines mark key  $\text{VO}_2(\text{M})$  peak positions.

The optical consequences are decisive: Figure 9 shows UV-Vis-NIR spectra of the oxidized sample at 30 and 100 °C. The near-identical curves confirm complete abolition of thermochromic switching [17]. This finding is consistent with reports that even partial V<sup>5+</sup> contamination can substantially suppress MIT sharpness, particularly in nanoparticle systems with high surface-to-volume ratios.

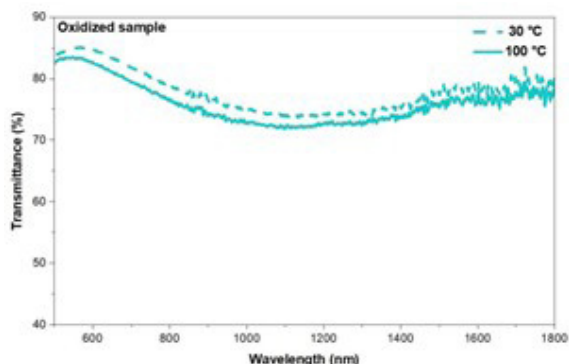


**Figure 9.** UV-Vis-NIR transmittance spectra of the oxidized sample at 30 °C (dashed line) and 100 °C (solid line). Near-identical curves confirm complete suppression of the thermochromic MIT.

Raman spectroscopy further corroborates the phase loss (Figure 10). The oxidized sample displays a featureless, monotonically rising background with no discernible VO<sub>2</sub>(M) phonon modes, consistent with a V<sub>2</sub>O<sub>5</sub>-dominated surface that lacks the characteristic V-V dimerization modes of the monoclinic lattice.

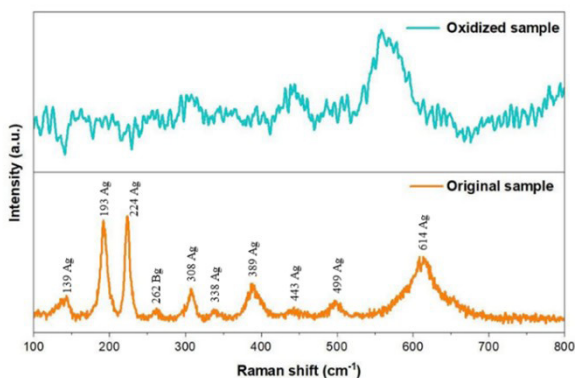


**Figure 10.** Raman spectrum of the oxidized VO<sub>2</sub> sample versus synthesized one. The featureless background and absence of VO<sub>2</sub>(M) modes confirm complete disruption of the monoclinic lattice.

### 3.3. Recovery of VO<sub>2</sub>(M) by thermal re-annealing

Re-annealing in Ar establishes a low oxygen partial pressure environment that suppresses re-oxidation of intermediate phases, enabling the thermally driven, stepwise lattice oxygen release sequence V<sub>2</sub>O<sub>5</sub> → V<sub>3</sub>O<sub>5</sub> → V<sub>4</sub>O<sub>9</sub> → V<sub>6</sub>O<sub>13</sub> → VO<sub>2</sub> to proceed without introducing unwanted dopants or secondary chemical reactions [18]. The phase evolution was tracked visually (Figure 11) and by XRD (Figure 12).

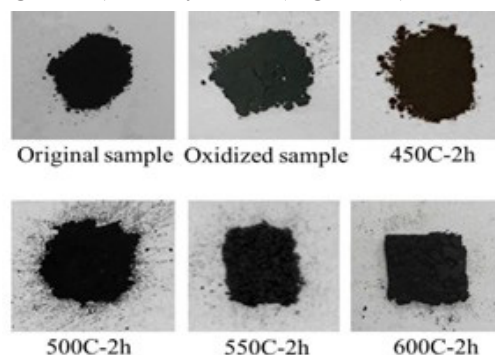


**Figure 11.** Optical photographs comparing original VO<sub>2</sub>(M), oxidized sample, and re-annealed samples at 450, 500, 550, and 600 °C (2 h each). The 500 – 600 °C samples recover the characteristic black color.

In Figure 12, re-annealing at 450 °C (black trace) yields broad, poorly resolved peaks with poor agreement to the VO<sub>2</sub>(M) reference - indicating incomplete reduction. At 500 °C (pink trace), a clean pattern matching the VO<sub>2</sub>(M) reference (red sticks) is obtained with no V<sub>2</sub>O<sub>5</sub> or VO<sub>2</sub>(B) impurities. At 550 °C and 600 °C, additional peaks inconsistent with VO<sub>2</sub>(M) appear, attributable to minor VO<sub>2</sub>(B) or over-reduced secondary phases. [18]

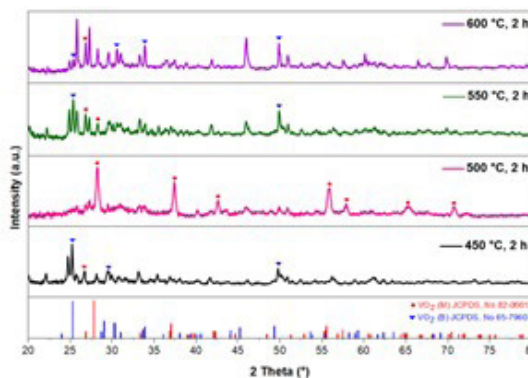


**Figure 12.** XRD patterns of samples re-annealed at 450 °C (black), 500 °C (pink), 550 °C (dark green), and 600 °C (purple), with VO<sub>2</sub>(B) (blue) and VO<sub>2</sub>(M) (red) reference patterns.

Raman spectroscopy of the 500 °C for 2 h sample, Figure 13 confirms the reappearance of sharp VO<sub>2</sub>(M) phonon modes at ~224 and ~614 cm<sup>-1</sup>, with additional features at ~139, ~193, ~262, ~308, ~338, ~389, ~443, and ~499 cm<sup>-1</sup>-all characteristic of the monoclinic lattice and V-V dimerization. No V<sub>2</sub>O<sub>5</sub> Raman bands are visible, providing unambiguous spectroscopic confirmation of complete phase recovery.

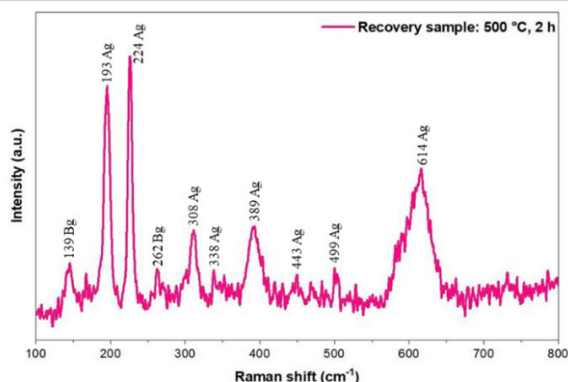


**Figure 13.** Raman spectrum of recovered VO<sub>2</sub>(M) (500 °C for 2 h). Characteristic VO<sub>2</sub>(M) modes at ~224 and ~614 cm<sup>-1</sup> are clearly restored.

### 3.4. Optimization of re-annealing duration

Comparing re-annealing at 500 °C for 2 h versus 3 h reveals a critical narrow processing window (Figure 14). The 2 h sample (left, pink) yields a phase-pure VO<sub>2</sub>(M) XRD pattern with no extraneous reflections. Extending the duration to 3 h (right, purple) introduces VO<sub>2</sub>(B) peaks (highlighted

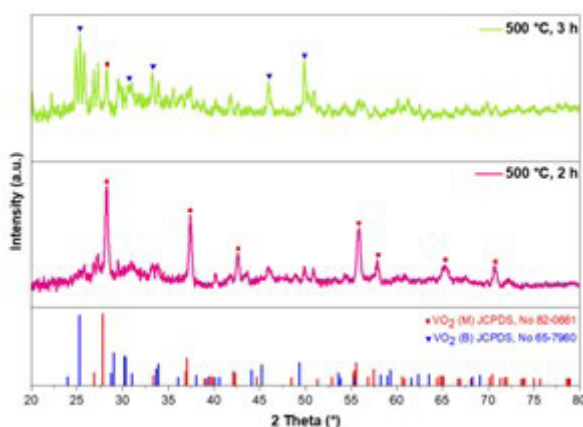


**Figure 14.** XRD comparison of re-annealing at 500 °C for 2 h (pink, left) and 3 h (lime green, right). The 3 h sample shows VO<sub>2</sub>(B) impurity peaks (dashed lines), confirming 2 h as optimal.

by dashed lines), indicating the onset of over-reduction or phase instability under prolonged thermal treatment. Therefore, 2 h is the optimal duration-sufficient for complete reduction yet short enough to avoid unwanted phase evolution.

### 3.5. Verification of thermochromic performance restoration

Figure 15 presents UV-Vis-NIR data for the optimally recovered sample (500 °C for 2 h). The spectra show a pronounced divergence between the 30 and 100 °C curves in the NIR region, fully restoring the thermochromic switching behavior of the original material. The recovered NIR contrast and switching temperature (~68°C) are quantitatively comparable to those of the original as-synthesized sample, with transmittance differences at 1800 nm of approximately 15% and 12.5% (~83.33%) for the original and re-annealed samples, respectively.

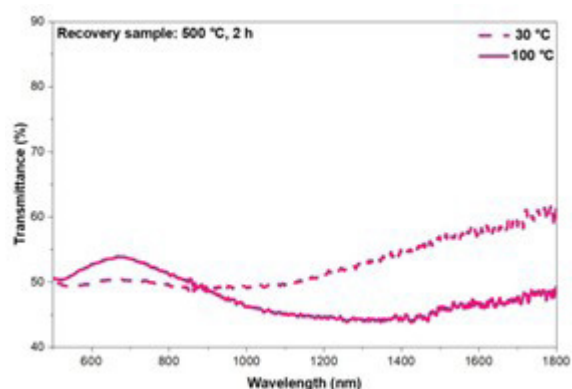


**Figure 15.** Characterization of recovered VO<sub>2</sub>(M) (500 °C for 2 h): UV-Vis-NIR transmittance spectra at 30 °C (dashed line) and 100 °C (solid line) confirming full thermochromic recovery.

The complete restoration of the MIT - a property exquisitely sensitive to stoichiometry, lattice order, and surface chemistry - confirms that re-annealing at the optimal condition drives thorough phase recovery, extending from the nanoparticle surface into the bulk. This result is consistent with previous reports on thin-film VO<sub>2</sub> systems where post-synthesis reduction treatments restored MIT sharpness and thermochromic contrast [2], [14], [19], [20]. The practical significance is considerable:

VO<sub>2</sub> nanoparticle synthesis requires multi-step procedures, specialized equipment, and expensive precursors. Rejuvenating oxidized stocks via a single 2-hour Ar annealing step - identical to the original synthesis annealing - eliminates the need to discard and resynthesize degraded material, reducing cost, waste, and synthesis time.

#### 4. CONCLUSION

This study has systematically demonstrated the feasibility of recovering phase-pure monoclinic VO<sub>2</sub>(M) nanoparticles from ambient-oxidized nanopowders through thermal re-annealing in argon. Progressive atmospheric oxidation converted V<sup>4+</sup> to V<sup>5+</sup>, yielding V<sub>2</sub>O<sub>5</sub> - rich phases that completely suppressed the MIT, as evidenced by XRD, Raman spectroscopy, and UV-Vis-NIR transmittance. Systematic re-annealing experiments across 450 – 600 °C and 2-3 h identified 500 °C for 2 h in Ar as the optimal recovery condition. Under these conditions, XRD and Raman spectroscopy confirmed complete VO<sub>2</sub>(M) phase restoration, and UV-Vis-NIR measurements verified quantitative recovery of thermochromic performance equivalent to the original as-synthesized nanoparticles. These results provide a practical, scalable protocol for extending the operational lifetime of VO<sub>2</sub> nanopowder batches, with direct implications for reducing material waste and cost in thermochromic device fabrication.

#### DECLARATION OF CONFLICTS OF INTEREST

*The authors declare that this research has no conflicts of interest.*

#### ACKNOWLEDGMENTS

*The authors gratefully acknowledge VLIR-UOS (Belgium) and Quy Nhon University for supporting this work under project codes VN2022IUC044A101 and S2025.1152.102. The authors also thank Hoang Nhat Hieu and Le Thi Thanh Lieu for SEM and XRD measurements.*

#### REFERENCES

- [1] P. Hu, T. D. Vu, M. Li, S. Wang, Y. Ke, X. Zeng, L. Mai, and Y. Long, "Vanadium Oxide: Phase Diagrams, Structures, Synthesis, and Applications," *Chemical Reviews*, vol. 123, no. 8, pp. 4353-4415, 2023.
- [2] J. Liu, Q. Li, T. Wang, D. Yu, and Y. Li, "Thermochromic VO<sub>2</sub> thin film prepared by post annealing treatment of V<sub>2</sub>O<sub>5</sub> thin film," *Advanced Materials Research*, vol. 79-82, pp. 747-750, 2009.
- [3] S. Liang, J. Shi, H. Zheng, B. Liu, Q. Liu, and C. Li, "A facile pathway to prepare VO<sub>2</sub> and V<sub>2</sub>O<sub>3</sub> powders via carbothermal reduction," *Journal of Solid State Chemistry*, vol. 265, pp. 299-305, 2018.
- [4] D. K. Manousou, E. Gagaoudakis, G. Michail, V. Binas, G. Kiriakidis, V. Diakonov, and M. Kompitsas, "VO<sub>2</sub> thin films fabricated by reduction of thermally evaporated V<sub>2</sub>O<sub>5</sub> under N<sub>2</sub> flow," *Materials Letters*, vol. 299, p. 130086, 2021.
- [5] Z. Yang, C. Ko, and S. Ramanathan, "Oxide electronics utilizing ultrafast metal-insulator transitions," *Annual Review of Materials Research*, vol. 41, pp. 337-367, 2011.
- [6] C. G. Granqvist, "Electrochromics for smart windows: oxide-based thin films and devices," *Thin Solid Films*, vol. 564, pp. 1-38, 2014.
- [7] M. M. Qazilbash et al., "Mott transition in VO<sub>2</sub> revealed by infrared spectroscopy and nano-imaging," *Science*, vol. 318, no. 5857, pp. 1750-1753, 2007.
- [8] A. Kumar, A. Kumar, A. Kandasami, and V. R. Singh, "A comprehensive review on synthesis, phase transition, and applications of VO<sub>2</sub>," *Journal of Superconductivity and Novel Magnetism*, vol. 37, no. 3, pp. 475-498, 2024.
- [9] J. Chen, X. Tian, L. Ye, P. Lu, Q. Luo, J. Yan, and D. Zhang, "High-performance VO<sub>2</sub> thin film prepared via room-temperature-deposition and air-annealing treatment," *Journal of Electronic Materials*, vol. 54, no. 9, pp. 7935-7941, 2025.

- [10] W. Burkhardt et al., "Tungsten and fluorine co-doping of VO<sub>2</sub> films," *Thin Solid Films*, vol. 402, no. 1-2, pp. 228-234, 2002.
- [11] Y. Gao, H. Luo, Z. Zhang, L. Kang, Z. Chen, J. Du, M. Kanehira, and C. Cao, "Nanoceramic VO<sub>2</sub> thermochromic smart glass: a review on progress in solution processing," *Nano Energy*, vol. 1, no. 2, pp. 221-246, 2012.
- [12] M. Soltani, M. Chaker, E. Haddad, R. V. Kruzelecky, and J. Margot, "Effects of Ti-W codoping on the optical and electrical switching of vanadium dioxide thin films grown by a reactive pulsed laser deposition," *Applied Physics Letters*, vol. 85, no. 11, pp. 1958-1960, 2004.
- [13] Y. Gao et al., "Enhanced chemical stability of VO<sub>2</sub> nanoparticles by the formation of SiO<sub>2</sub>/VO<sub>2</sub> core/shell structures and the application to transparent and flexible VO<sub>2</sub>-based composite foils with excellent thermochromic properties for solar heat control," *Energy & Environmental Science*, vol. 5, pp. 6104-6110, 2012.
- [14] Z. Zhang, Y. Gao, Z. Chen, L. Kang, H. Luo, "Thermochromic VO<sub>2</sub> Thin Films: Solution-Based Processing, Improved Optical Properties, and Lowered Phase Transformation Temperature," *Langmuir* vol. 26, pp. 10738-10744, 2010.
- [15] Z. Liang et al., "Long-term stability and efficiency of VO<sub>2</sub> nanostructure-based thermochromic smart windows," *ACS Applied Nano Materials*, vol. 7, no. 18, pp. 21683-21691, 2024.
- [16] Y. Yang et al., "Suppression of photoinduced surface oxidation of vanadium dioxide nanostructures by blocking oxygen adsorption," *ACS Omega*, vol. 4, no. 18, pp. 17735-17740, 2019.
- [17] J. Cao et al., "Strain engineering and one-dimensional organization of metal-insulator domains in single-crystal vanadium dioxide beams," *Nature Nanotechnology*, vol. 4, no. 11, pp. 732-737, 2009.
- [18] Y. Ningyi, L. Jinhua, L. Chenglu, "Valence reduction process from sol-gel V<sub>2</sub>O<sub>5</sub> to VO<sub>2</sub> thin films," *Applied Surface Science*, vol. 191, no. 1-4, pp. 176-180, 2002.
- [19] M. Kumar, S. Rani, J. P. Singh, K. H. Chae, Y. Kim, J. Park, and H. H. Lee, "Structural phase control and thermochromic modulation of VO<sub>2</sub> thin films by post thermal annealing," *Applied Surface Science*, vol. 529, pp. 147093, 2020.
- [20] S. Wang, M. Liu, L. Kong, Y. Long, X. Jiang, and A. Yu, "Recent progress in VO<sub>2</sub> smart coatings: strategies to improve the thermochromic properties," *Progress in Materials Science*, vol. 81, pp. 1-54, 2016.



© 2026 by the authors. This Open Access Article is licensed under the Creative Commons Attribution-NonCommercial 4.0 International (CC BY-NC 4.0) license (<https://creativecommons.org/licenses/by-nc/4.0/>).

# Phục hồi pha tinh thể đơn tà của hạt nano $VO_2$ từ mẫu bị oxy hóa: đánh giá khả năng tái sử dụng và tối ưu điều kiện nung phục hồi

Hồ Nguyễn Hồng Thắm<sup>1</sup>, Nguyễn Thị Thanh Nhân<sup>1</sup>, Nguyễn Thị Tường Vy<sup>1</sup>,  
Lê Phương Thảo<sup>1</sup>, Lê Thị Mỹ Nhi<sup>2</sup>, Hoàng Thị Hằng<sup>2,3</sup>, Lê Thị Ngọc Loan<sup>2,\*</sup>

<sup>1</sup>Khoa Sư phạm, Trường Đại học Quy Nhơn, Việt Nam

<sup>2</sup>Khoa Khoa học Tự nhiên, Trường Đại học Quy Nhơn, Việt Nam

<sup>3</sup>Khoa Vật lý và Thiên văn học, Đại học KU Leuven, Vương quốc Bỉ

Ngày nhận bài: 27/02/2026; Ngày sửa bài: 24/03/2026;

Ngày nhận đăng: 25/03/2026; Ngày xuất bản: 28/06/2026

## TÓM TẮT

Các hạt nano vanadium dioxide ( $VO_2$ ) pha đơn tà (M) có khả năng chuyển đổi pha giữa kim loại - bán dẫn (MIT) thuận nghịch tại  $\sim 68^\circ C$  đã mở ra các ứng dụng nhiệt sắc như cửa sổ thông minh và cảm biến nhiệt. Tuy nhiên, việc phơi nhiễm trong môi trường khí quyển gây ra hiện tượng oxy hóa bề mặt, chuyển đổi  $V^{4+}$  thành  $V^{5+}$ , dẫn đến suy giảm chất lượng pha tinh thể hoặc thay đổi thành phần pha làm mất chức năng nhiệt sắc. Trong nghiên cứu này, các hạt nano  $VO_2$  bị oxy hóa cho thấy khả năng được phục hồi hoàn toàn bằng cách nung lại trong môi trường khí trơ. Từ các hạt nano  $VO_2(M)$  được tổng hợp bằng phương pháp thủy nhiệt, quá trình oxy hóa được thực hiện trong điều kiện môi trường không khí tạo ra mẫu có chất lượng tinh thể bị suy giảm và chứa thành phần  $V_2O_5$ . Để khảo sát khả năng hồi phục pha tinh thể  $VO_2(M)$ , quá trình nung lại được khảo sát một cách hệ thống từ  $450 - 600^\circ C$  trong 2-3 giờ, kết quả cho thấy nung ở điều kiện tại nhiệt độ  $500^\circ C$  trong 2 giờ là điều kiện phục hồi tối ưu. Phép phân tích XRD, phổ Raman và đo phổ truyền qua UV-Vis-NIR cho thấy  $VO_2(M)$  khôi phục hoàn toàn pha và hiệu suất nhiệt sắc gần tương đương với vật liệu ban đầu.

**Từ khóa:** Vanadium dioxide, cửa sổ thông minh, vật liệu chuyển pha, hồi phục tính chất nhiệt sắc.

\*Tác giả liên hệ chính.

Email: lethingocloan@qnu.edu.vn